Anal. Bioanal. Electrochem., Vol. 11, No. 4, 2019, 484-496

Analytical & Bioanalytical Electrochemistry

2019 by CEE
www.abechem.com

Full Paper

A Novel Sensitive Label-free Impedometric Electrochemical Immunosensor for Detection of t-NMP22 using FFT Square Wave Voltammetry

Alireza Bonakdar,[1] Mohamad Javad Rasaee,[1] Saman Hosseinkhani[2],* Fatemeh Rahbarizadeh[1] and Fereidoun Mahboudi[3]

[1]Department of Medical Biotechnology, Faculty of Medical Sciences, Tarbiat Modares University, Tehran, Iran
[2]Department of Biochemistry, Faculty of Biological Sciences, Tarbiat Modares University, Tehran, Iran
[3]Biotechnology Research Center, Pasteur Institute of Iran, Tehran, Iran

*Corresponding Author, Tel.: +982182884407; Fax: +982188009730
E-Mail: saman_h@modares.ac.ir

Received: 10 January 2019 / Received in revised form: 9 March 2019 / Accepted: 10 April 2019 / Published online: 30 April 2019

Abstract- It is known truncated Nuclear matrix protein 22 (t-NMP22) could be used a biomarker for Bladder cancer. Therefore, in this paper a highly sensitive electrochemical technique was developed based on nanostructures modified glassy carbon (GC) electrode for detection of t-NMP22. In this measurement, immunosensor was fabricated based on the electrodeposition of gold in general the upper frequency limit is determined by the solution resistance, which depends on the specific conductivity of the electrolyte and the electrode radius. To increase the sensitivity of the electrochemical system for detection of t-NMP22, the most important parameters were optimized. The fabrication steps of the immunosensor were characterized by cyclic voltammetry and electrochemical impedance spectroscopy. FFT square wave voltammetry (FFTSWV) was used for measurements at optimum condition. Moreover, the effect of important parameters such pH the FFTSWV parameters were investigated. The modified electrode was used for determination of different concentrations of t-NMP22; a linear range from 0.05 ng/mL to 30 ng/mL and a detection limit of 16.4 pg/mL were obtained. The proposed detection technique does not need a redox probe and was evaluated in urine, which showed good selectivity, high sensitivity and stability, reproducibility.

Keywords- t-NMP22, Label-free immunosensor, Gold nanoparticles, FFT square wave voltammetry

---

1. INTRODUCTION

t-NMP22, defined as truncated nuclear matrix protein 22, has been introduced as a urinary biomarker by Food and Drug Administration (FDA), which could be helpfully used for the detection of bladder cancer (BC) [1, 2]. As unfortunately the type of cancer has growing trend nowadays, t-NMP22 immunoassay beside combined classic techniques such as cytology have triggered intense attention and there are numerous recorded reports on this topic [3-5].

It is believed that since classic methods such as cytology and cystoscopy confront obstacles like being expensive, invasive or having discomfortable monitoring process for the patients and limitations as low sensitivity beside notable variability and the interpretation of urine samples, which strongly is associated with the cytology expert [3,6]. On the other hand, cystoscopy sensitivity is severely grounded to the visualized tumor so that flat in situ carcinomas could be easily ignored [7]. Among classic methods, ELISA could have the adequate sensitivity, it has deficiencies of being multi-steps and highly time consuming, and thus it would not have the potential to be used for large sample scales or rapid detection [8,9].

Since there happens an important immunological reaction between the protein agent and the related antigen, immunoassay have found a unique place in the field and various types of immunosensors are being broadly developed and employed as an analytical method in blood or body biological fluids [10,11]. Particularly, electrochemical immunosensors have achieved critical place for biomarkers detection generally both in human or plant diseases and this can surely be because of their high excellent specificity, high selectivity and sensitivity, quick response, low cost, and simple procedures in comparison with conventional methods such as cystoscopy [10-12].

The most important key factor in the preparation of immunosensor is this that the right method must be chosen to employ for immobilization antibody onto electrode surface so it strongly would help their activity to be maintained at higher levels and also the electron transfer could be assisted to be done easier through the redox process at the electrode surface [13,14]. On this purpose, compounds that are terminated with thiol groups such as mercapto materials can be strongly be immobilized onto the surface of solid state electrode like gold electrode via self-assembled monolayers (SAM) formation [15,16].

The other advantage is about electrochemical immunosensor specifically the label-free type is that they have the ability to be modified by nanomaterials [10]. For instance, Au NPs can successfully absorb biological complex being highly active and immunosensors based on the antigen/antibody immunocomplex at the electrode surface has also been noticed among recent reports [17,18].

The aim of this work is to present a new electrochemical method using a label free immunosensor for detection of t-NMP22 based on selective adsorption of the analyte on the electrode, wherein the immobilized antibodies t-NMP22 carried out on the modified AuNPs/GC by self-assembly of 3-Mercaptopropionic acid (MPA), 11-Mercaptoundecanoic

acid (MUA) and bovine serum albumin (BSA). For detection, the interaction of antibody and NMP22 antigen at the surface of the immunosensor produce the electrochemical signal for the analyte was obtained by FFT SW voltammetry. Also, the electrode surface was studied by cyclic voltammetry (CV) and electrochemical impedance spectroscopy (EIS).

2. EXPERIMENTAL

2.1. Preparation of rGO

$K_3Fe(CN)_6$, $K_4Fe(CN)_6$, KCl 11-Mercaptoundecanoic acid (MUA) 95%, 3-Mercaptopropionic acid (MPA) 96%, N-Hydroxy Succinimide (NHS), Tween-20NHS, 98% N-(3-Dimethylaminopropyl)-N′-ethyl carbodiimide hydrochloride (EDC), 3-Mercapto Propionic acid (MPA) 99%, and bovine serum albumin (BSA), were obtained from Sigma-Aldrich. The chemicals were in analytical grade. Phosphate buffer solution (PBS) containing Na_2HPO_4, KH_2PO_4 was prepared. Also, Phosphate buffer solution 0.05% w/v Tween 20 (PBST) was prepared in double distilled water. The analyte, was the first 300 amino acids of NMP22 is named truncated (t-NMP22), which was selected based on "In silico" studies and reported data [19], as following sequence;

MTLHATRGAALLSWVNSLHVADPVEAVLQLQDCSIFIKIIDRIHGTEEGQQILKQP
VSERLDFVCSFLQKNRKHPSSPECLVSAQKVLEGSELELAKMTMLLLYHSTMSSKSP
RDWEQFEYKIQAELAVILKFVLDHEDGLNLNEDLENFLQKAPVPSTCSSTFPEELSPP
SHQAKREIRFLELQKVASSSSGNNFLSGSPASPMGDILQTPQFQMRRLKKQLADERSN
RDELELELAENRKLLTEKDAQIAMMQQRIDRLALLNEKQAASPLEPKELEELRDKNE
SLTMRLHETLKQCQ

In this research, the antibody against t-NMP22 (Ab) was prepared based on the reported method [20,21].

2.2. Fabrication steps of the Immunosensor

For the fabrication of the immunosensor, at first, the GCE was polished with 0.3 μm and 0.05 μm alumina powders, respectively, and then, cleaned ultrasonically in 0.01 M NaOH solution and dried with blowing N_2. AuNPs/GC electrode was constructed by deposition of AuNPs on the electrode surface. The electrode was place in solution containing 5.0 mg/ml^{-1} $HAuCl_4$ and 0.1 M $NaNO_3$, 200 s at -200 mV. Then, to obtain MUA/MPA-AuNPs/Au, AuNPs/Au electrode was immersed in 3 mM MUA/MPA (7:3; v/v) in ethanol solution, and the electrode was rinsed with ethanol and water to remove unbound MUA-MPA. Next, the electrode was immersed in 400 mM EDC and 100 mM NHS solution of for 90 min to form NHS esters; it was rinsed with deionized water. Afterward, 20 μL of mAb0.5 mg/ml solution in PBS was casted on EDC/NHS/MUA-MPA/AuNPs/GC and incubated for 90 min and rinsing

with PB solution. At the end, the electrode was incubated in 1% BSA and PBTS to block the unreacted carboxylic groups and non-specific sites.

After washing, the electrode with ultrapure water, it was incubated in BSA solution (1%, w/w) for 90 min to block existing free sites. Finally, electrode was washed and stored at 4 °C prior to use mAb/EDC/NHS/MUA-MPA/AuNPs/GC immunosensor was used for measurement of t-NMp22. At first 20 µL of t-NMP22 solutions concentrations in range of 0.04 to 50 ng/mL was casted on the immunosensor, and it was incubated for 1 h at 37 °C, and then, it was washed with PBS. The method used for obtaining electrochemical signal was differential DFFTSWV. Where, the immunosensor signal was measured before and after casting t-NMP22 solutions. The impedance differences (ΔZ) of two voltammogram peaks were used as the immunosensor response. Fig. 1 represents the immunosensor fabrication steps.

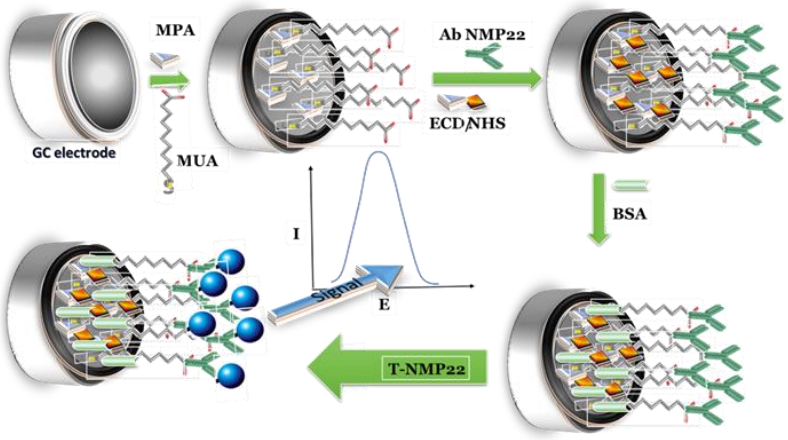

Fig. 1. The steps presentation of the t-NMP22 immunosensor fabrication

2.3. Instrumentation

FFTSWV measurements were performed by a homemade potentiostat, and software was used to control it via an A/D board (PCL-818H, Advantech Co.) [22, 23]. The electrochemical software was developed in our lab to applied potential waveform on a cell, which contain three-electrodes: Ag/AgCl reference electrode, a platinum wire as the auxiliary electrode the working electrode. Also, the electrochemical program was employed to acquire current readings, processed and plotted the data. The potential step (E_c) in the potential waveform, was operated for conditioning the electrode, which follows by a multiple SW pulses cycles (were superimposed on a staircase potential) with an amplitude of E_{sw} and frequency of f_o. The staircase potential was changed by a small potential step of ΔE. The values of potential pulse of SW (E_{sw}) and ΔE values were in a range of few mV (10 to 50 mV). The EIS measurements AutoLab Potentiostat PGSTAT302N (Metrohm AutoLab, Utrecht) was used (at frequency range from 0.1 Hz to 1 MHz, at a DC potential of 0.2 V and AC amplitude of 0.01 V). Cyclic voltammetry (CV) and SW measurements, was a homemade potentiostat.

2.4. Real samples

The urine of five different patients and healthy were obtain as samples, and stored at -20 °C until use. Also, RT-PCR analysis was performed in order to confirm the presence of t-NMP22 in the urine samples.

3. RESULTS AND DISCUSSION

3.1. SEM Characterization of the electrode surface

For study of the morphology of the modified GC electrode by deposition of Au NPs, SEM method was used. As shown the SEM in Fig. 2A, the GC electrode has a clean and smooth surface. Fig. 2B shows the electrode surface after deposition of gold NPs, in which the Au NPs with an average particle size of 85 nm (see Fig. 3C). As seen, the Au NPs have a good distribution, which could help increase the surface area of the electrode, and consequently, the amount of immobilized antibody. In this image, the deposition time of AuNPs was 300 s periods, in which a smaller size particles but with higher density can be obtained.

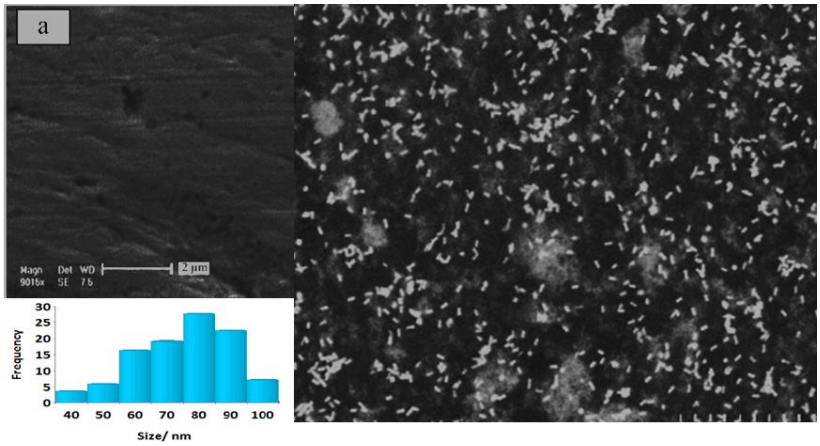

Fig. 2. SEMs picture of A) GC electrode; B) modified GC electrode, and C) the size distribution histograms, and D) AuNPs/GC

3.2. Electrochemical Characterization of the immunosensor

Cyclic voltammetry and EIS were used to study of the immunosensor during each fabrication steps of mAb/ EDC/NHS/MUA-MPA-AuNPs/GC. In the most popular formats for evaluating impedance Z(t) is the Nyquist and Bode plots. In the former format, the imaginary impedance component (Z") is plotted against the real impedance component (Z') at each excitation frequency, whereas in the latter format, both the logarithm of the absolute impedance, |Z| and the phase shift, Ë, of the impedance, are plotted against the logarithm of the excitation frequency. Fig. 3, A and B illustrate the voltammograms and EIS curves.

As shown, the spectrums (known as Nyquist plots) in Fig. 3B, the impedance for the modification steps of the GC electrode at frequency range 0.1 Hz to 1 MHz with AC amplitude

of 10 mV, and DC potential of 200 mV. Due to this fact that, the semicircle diameter at higher frequencies in the Nyquist plot corresponds to the R_{ct}, and at lower frequencies corresponds to the changes in diffusion process (linear part) In Fig. 3B, at bare AuNPs /GC electrode, (curve a) has a small semicircle diameter, which correspond to a small R_{ct} (1kΩ) . This implies higher conductivity along with a substantial diffusion for $[Fe(CN)_6]^{3-/4-}$ ions at the electrode surface (straight line). Also, the corresponding CV in Fig. 3B (curve a), a pair of well-defined reversible peaks can be seen in the cyclic voltammogram of redox reaction of $[Fe(CN)_6]^{3-/4-}$ for the AuNPs/GC electrode.

But, in case of MUA-MPA/AuNPs/GC electrode, Fig. 3A (curve b) shows the calculated value of R_{ct}, is significantly increased to 3.9 kΩ. This could be due to formation of SAM on the electrode surface, and the charge repulsive interaction between of carboxylic groups on the SAM and $[Fe(CN)_6]^{3-/4-}$ ions, which can limit the diffusion of $[Fe(CN)_6]^{3-/4-}$ ions at the electrode surface. Also in Fig. 3B,

The activation the formed monolayer with EDC/NHS causes reduction in the value of R_{ct} clearly to 1.4 kΩ. Curve b shows the result was obtained for the EIS measurement. Fig. 3A (curve c), also, displays the voltammogram for EDC/NHS/MUA-MPA/AuNPs/GC electrode, which displays an increase in the peaks current. Also, the current enhancement could be related to two issues. The current enhancement could be referred to the conversion of the COO^- terminal groups of MUA-MPA layer to NHS esters. This could diminishes the repulsive interaction between $[Fe(CN)_6]^{3-/4-}$ ions EDC/NHS/MUA-MPA/AuNPs/GC, which results into the increase in the diffusion of $[Fe(CN)_6]^{3-/4-}$ ions.

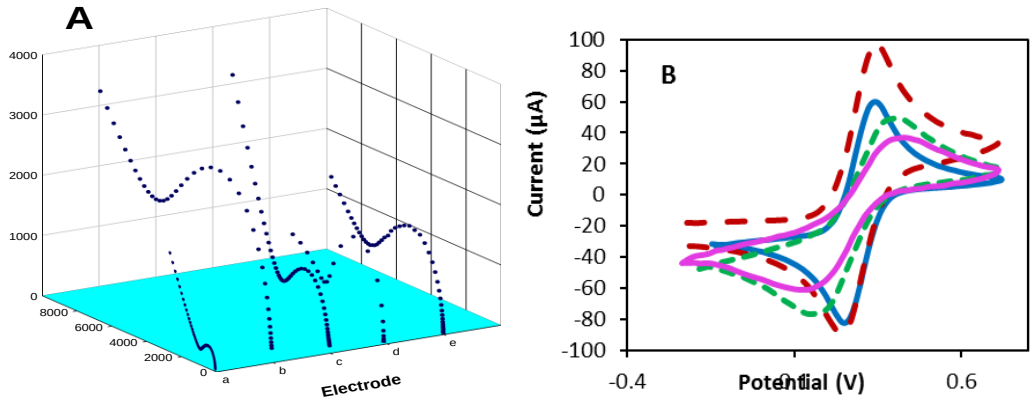

Fig. 3. A) Nyquist plots for (a) bare AuNPs/GC, (b) MUA-MPA/AuNPs/GC, (c) EDC/NHS-MUA-MPA/AuNPs/GC, (d) mAb/MUA-MPA AuNPs/GC, (e) t-NMP22- mAb/ EDC/NHS-MUA-MPA/AuNPs/GC at AC frequency range 0.1 Hz to 1 MHz, DC potential of 100 mV and AC amplitude of 10 mV; **B**) Cyclic voltammograms for (A) bare AuNPs/GC, (B) MUA-MPA/AuNPs/GC, (c) EDC/NHS-MUA-MPA-AuNPsAuNPs/GC, (d) mAb/EDC/NHS/MUA-MPA/AuNPs/GC, (e) t-NMP22 mAb/EDC/NHS/MUA-MPA/AuNPs/GC at scan rate 40 mVs^{-1}, in PB solution, pH 7.5, containing 400 mM KCl, 5 mM $[Fe(CN)_6]^{3-/4-}$

In the case EDC/NHS/MUA-MPA/AuNPs/GC, in Fig. 3A (curve d), addition layers of mAb/ EDC/NHS/MUA-MPA-AuNPs/GC, the EIS curve (d) shows an enhancement in the value of R_{ct} in which it is to 3.1 kΩ. Also, in Fig. 3B (curve d), the recorded cyclic voltammograms shows a drop in the value of peak current, which is an indication of the formation a bound between mAb and EDC/NHS/MUA-MPA/AuNPs/GC. And finally the curve e shows the attachment between the t-NMP22 and mAb/EDC/NHS/MUA-MPA/AuNPs/GC.

3.3. Determination of the electrode signal

The EIS experiments show that there is a response of an electrochemical cell to AC waveform or small amplitude sinusoidal voltage signal as an excitation function of frequency. The response current is a sine wave, which has a phase shift respect to the original potential wave. While the value of impedance (Z(t)) is equal to E(t)/I(t). The value of Z(t) is usually expressed as a complex number, where the ohmic reactance is the real component and the capacitive reactance is the imaginary response. In the FFTSWV measurements, the analyte signal is the change of the impudence of the electrode during adsorption of t-NMP22 on mAb/EDC/NHS-MUA-MPA/AuNPs/GCE surface. Where the electrode response depends on the, electrode kinetics of the molecular interactions at the immunosensor could be considered analogous to the impudence components, which is result of the electron transfer blocking. However, in case of adsorption, the value of the double layer capacitance will changed due to the change in the dielectric constant or the thickness of the capacitance layer. The formation of biochemical reaction products may be represented by an additional capacitor that depending on the process may be included in parallel or in series with the double-layer capacitor The solution Z(t) of the electrode is related to the reactance of the double layer by:

$$Z(t) = -\frac{j}{\pi r_0^2 \omega C_{dl}} \tag{1}$$

Where r_o is the electrode radius, C_{dl} is the double layer capacitance of the electrode. As mentioned above, in FFTSWV the currents were sampled four times in one SW cycle (i_0, i_1, i_2 and i_3), in each step, ΔE, of staircase potential ramp. Then, the in the computer memory data were stored in an array matrix.

To calculate the admittance of the detector response, first the real and imaginary components of the alternating of current need to be calculated. The real component of *I'* and *E'* are given by,

$$I' = i_2 - i_0 \tag{2}$$

$$E' = E_2 - E_0 = -2Es \tag{3}$$

and the imaginary components were calculated,

$$I'' = i_1 - i_3 \quad (4)$$

$$E'' = E_1 - E_3 = 2Es \quad (5)$$

$$Z(t) = -\frac{I''-JI'}{E'-jE''} \quad (6)$$

In fact, in the absence of a redox pair, (no faradic process occurs) value of rate the charge transfer on the electrode is very small. Based on the equation (6), it is possible to calculate Z(t), which is strongly depends on the analyte adsorption. The effect of the analyte concentration on the value of impedance of the electrode in PBS is shown in Fig. 4. As shown there is relationship between Z(t) and the analyte concentration. However, in order to obtain maximum response the most important parameters were optimized.

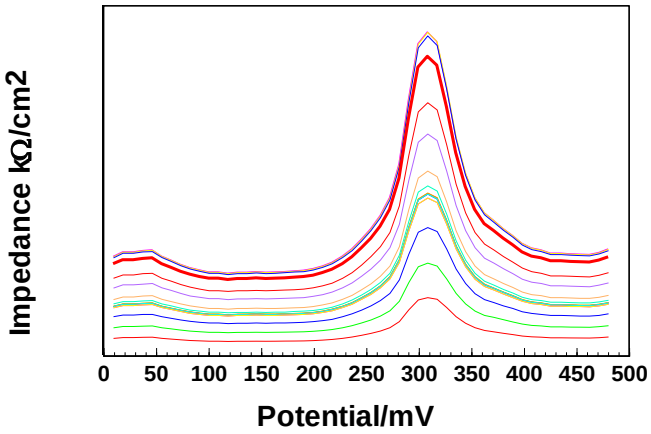

Fig. 4. Impedance voltammograms of mAb/EDC/NHS/MUA-MPA/AuNPs/GCelectrode in PB solution, pH 7.4, containing 400 mM KCl, after incubation with (a-h) 50 pg/ml, 100 pg/ml, 300 pg/ml, 500pg/ml, 1 ng/ml, 5 ng/ml, 10 ng/ml, 20 ng/ml of t-NMP22, in the potential range of 0 to 500 mV at frequency of 250 Hz and amplitude of 20 mV

3.4. Optimization of the parameters

The adsorption of the analyte on mAb/EDC/NHS/MUA-MPA/AuNPs/GC surface reported a detection method by using FFTSW. Once FFTSWV is used to measure, t-NMP22 electrochemical processes will cause a measurable change in the impedance voltammogram. In order to find the optimum conditions for the analytical measurement numerous SW were done. The first parameter examined were the SW frequency and amplitude in rang of 10 t0 500 Hz and 5 t0 50 mV. The results of measurement of S/N for concentration of 60 pg/ml solution are shown in Fig. 5A. As shown in the figure, the value of signal/noise ratio (S/N) increases with the frequency up to 300 Hz and then decreased with frequency. It is possible at low the

frequencies, a longer time for paling the potential allows to adsorb more analyte from the solution on the electrode surface, the active surface also increased S/N. But, the upper of the signal is limited by the solution resistance; the highest applied frequency depends on the specific conductivity of mAb/EDC/NHS/MUA-MPA/AuNPs/GC surface and the electrolyte. Therefore, in the figure the maximum S/N is seen in amplitude of 35 mV, and frequency of 300 Hz.

The value pH of the buffer solution also is one of the most important, which can affect the electrode response, or the activity of immobilized antibodies. Consequently, to discover the best pH, the immunosensor response (ΔZ) was measured by changing the pH of the buffer in the range from 5 to 8.0. As shown in Fig. 4B the change in the value of S/N with pH values. The graph indicates that the incensement of pH up to 7.4 causes the S/N and then it declines at higher pH values. This could be related to the instability of immunosensors in higher or lower pHs. Accordingly, the value of pH 7.4 was selected for the measurements.

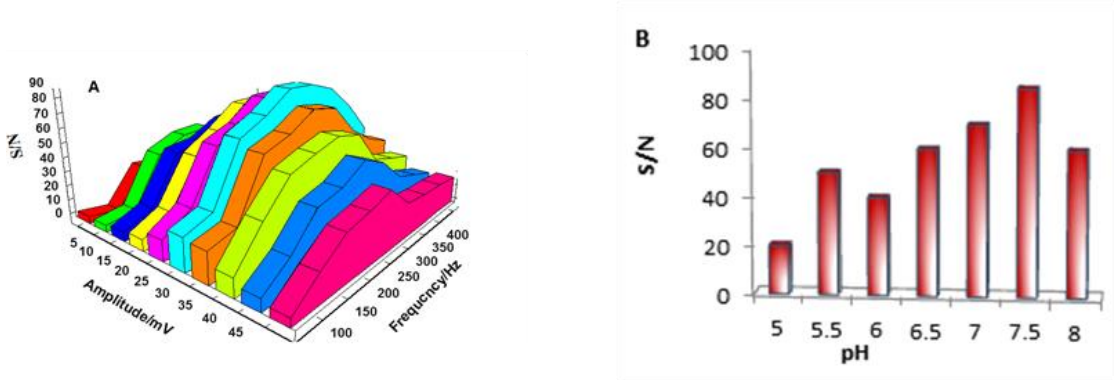

Fig. 5. (A) The effect of frequency and amplitude in the potential range of 0 to 500 mV on the electrochemical response of the immunosensor to of t-NMP22 200 pg/ml in PB solution, pH 7.5, containing 400 mM KCl and (B) The of pH on the response

3.5. Calibration curve

For determination of t-NMP22 by the FFTAV, mAb/EDC/NHS/MUA-MPA/AuNPs/GC in PBS was incubated in set of standard solutions of t-NMP22 c in the range of concentrations 50 pg/ml to 50 ng/ml. Then the value of ($\Delta Z=Z(t) - Z_0$) of the electrode was obtained, where Z(t) is the impedance of the analyte after incubation of the electrode in different concentrations standard solutions of t-NMP22 and Z_0 is the impedance peak of the immunosensor before incubation. Fig. 6 shows the calibration curve which has the electrode response different concentrations and of the analyte. As displayed, the value of the ΔZ of the electrode is proportional to the t-NMP22 concentration. In fact, the plateau section of the concentration curve for t-NMP22 with the response is an indication of the adsorption of the analyte at the electrode surface.

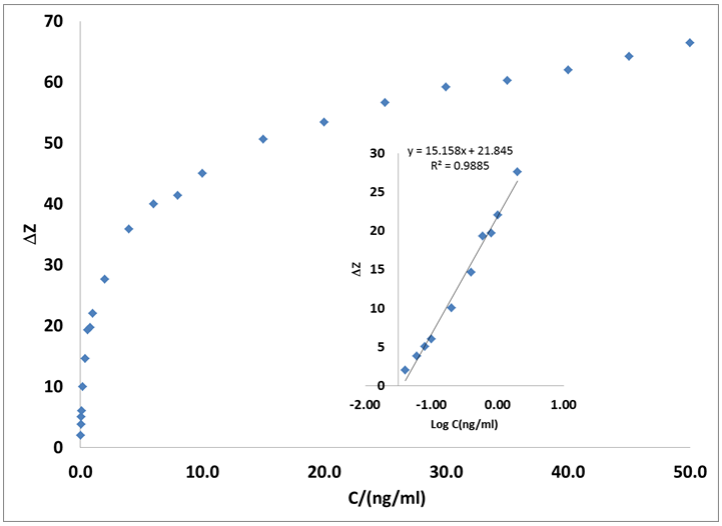

Fig. 6. The differentiated FFT impedance response of mAb/EDC/NHS/MUA-MPA/AuNPs/GC electrode after incubation with (a-h) 0.04 to 50 ng/ml of t-NMP22 B) Linear relationship between ΔR (kΩ) and concentrations t-NMP22 in the range of 0.04 nM to 30 ng/ml. The inset shows log relationship between ΔZ (k Ω) and concentrations the in the same range

The inset curve in Fig. 6 displays the calibration in form of the immunosensor responses versus concentrations of t-NMP22, in the range of 0.04 to 50 ng/ml. As shown, the linear line a relationship between the response and logarithm of concentrations t-NMP22 must be considered, which confirm the adsorption process of the analyte on the electrode surface.

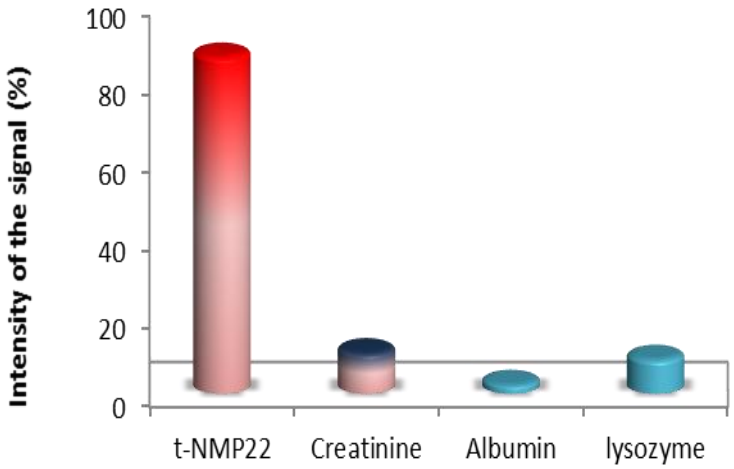

Fig. 7. Signal impedance percentages change when interfering compounds, albumin, lysozyme and creatinine) at 1.0 ng/mL and t-NMP22 were measured with mAb/EDC/NHS/MUA-MPA/AuNPs/GC

The equation for the linear curve is ΔZ=15.158 log C (ng/ml)+21.485 with a correlation coefficient of 0.98852 and %RSD of 4.85% (n=3). Also, the calculated detection limit (LOD) for the method is 16.4 ng/ml.

3.6. Selectivity of the immunosensor

In order to test the selectivity of the immunosensor toward the presence of possible interferences, set high concentrations of albumin, lysozyme and creatinine in urine species in the real samples was measured by FFTSW voltammetry. Fig. 7 demonstrates the immunosensor response of the selected interference, and the t-NMP22. These results as shown, the selectivity of the immunosensor is approved and acceptable.

The immunosensor was tested in the determination of t-NMP22 in artificially urine. Therefore, a set of standard solution of t-NMP22 were spiked into the samples solution. Also, in the processes of t-NMP22 detection in the real samples, 15 µl of urine containing 0, 200 and 600 pg/mL of t-NMP22 was used in, then the electrode response was measured. As seen in Table 1, the data demonstrates a good performance.

Table 1. The results of measurement of t-NMP22 by immunosensor in urine

Urine sample	Urine (µL)	t-NMP22 added (ng/mL)	Δ Z	t-NMP22 found (ng/ml	Recovery (%)
1	2	–	4.50	5.11±0.1	
2	2	2	8.12	7.21±1.2	96.1
3	2	4	12.3	17.11±1.12	95.2

Table 2. Comparison of different t- NMP22 electrochemical immunosensors

Electrode materials	Linear range (U/mL)	Detection limit	Ref.
Au@Pd/Agyolk-bimetallic shell nanoparticles and amination graphene	0.01 to 18 ng/mL	3.3 pg/ml	[24]
reduced graphene oxide–tetraethylene pentamine and trimetallic AuPdPt	0.040 to 20 U/ml	1 U/ml	[25]
t-NMP22/mAb / MUA-MPA AuNPs/GC electrode	0.04–20 ng/ml	16.4 pg/ml	This work

The comparison of t-NMP22/antibody-NMP22/ MUA-MPA AuNPs/GC electrode sensor with the other immunosensors is shown in Table 2. As seen, the detection limit of this immunosensor is acceptable, and it also has a wider linear range. These indicated, the proposed detection system provides a good recognition platform for t-NMP22, which has a promising application in clinical devices.

4. CONCLUSION

Due to this fact that t-NMP22 is shown as biomarker for the bladder cancer. Therefore, it is very attractive case for researcher to establish new sensitive and selective detection method for the maker. In this direction here, it was attempted to develop an immunosensor for t-NMP22, in which mAb/MUA-MPA/AuNPs/GC was used for an impedometric measurements. The immunosensor was presented a good response toward the t-NMP22, due to modification of the electrode, which provided selectivity and increases the number of available effective binding sites. The combination of immunosensor and FFT SWV here may be used in construction a prototype device for screening that is very helpful for early detection of the cancer.

Acknowledgements

The authors would like to thank Tarbiat Modares University and Research Council of University of Tehran for financial supporting of this research.

REFERENCES

[1] A. Bonakdar, M. J. Rasaee, S. Hosseinkhani, F. Rahbarizadeh, F. Mahboudi, and M. R. Ganjali, Int. J. Electrochem. Sci 14 (2019) 3168.

[2] W. Zhuge, X. Tan, R. Zhang, H. Li, and G. Zheng, Chinese Chem. Lett. (2019). https://doi.org/10.1016/j.cclet.2019.02.026Get rights and content.

[3] S. Zhao, Y. Zhang, S. Ding, J. Fan, Z. Luo, K. Liu, Q. Shi, W. Liu, and G. Zang, J. Electroanal. Chem. 834 (2019) 33.

[4] D. D'Andrea, F. Soria, S. Zehetmayer, K. M. Gust, S. Korn, J. A. Witjes, S. F. Shariat, BJU international (2019). doi: 10.1111/bju.14673.

[5] M. Perera, S. McGrath, S. Sengupta, J. Crozier, D. Bolton, and N. Lawrentschuk, Nature 41585 (2018) 018-0066.

[6] T. A. Longo, S. C. Brousell, and B. A. Inman, Urine Cytology and Existing Urinary Biomarkers for Bladder Cancer, Precision Molecular Pathology of Bladder Cancer, Springer (2018) pp. 137-155.

[7] S. F. Shariat, M. J. Marberger, Y. Lotan, M. Sanchez-Carbayo, C. Zippe, G. Ludecke, H. Boman, I. Sawczuk, M.G. Friedrich, R. Casella, C. Mian, S. Eissa, H. Akaza, V. Serretta, H. Huland, H. Hedelin, R. Raina, N. Miyanaga, A. I. Sagalowsky, C. G. Roehrborn, P. I. Karakiewicz, J. Urolog. 176 (2006) 919.

[8] J. March-Villalba, J. Panach-Navarrete, M. Herrero-Cervera, S. Aliño-Pellicer, and J. Martínez-Jabaloyas, Actas Urológicas Españolas 42 (2018) 524.

[9] S. K. Arya, and P. Estrela, Biosens. Bioelectron. 117 (2018) 620.

[10] H. Haji-Hashemi, M. M. Habibi, M.R. Safarnejad, P. Norouzi, and M. R. Ganjali, Sens. Actuators B 275 (2018) 61.
[11] H. Haji-Hashemi, M. R. Safarnejad, P. Norouzi, M. Ebrahimi, M. Shahmirzaie, and M. R. Ganjali, Anal. Biochem. 566 (2019) 102.
[12] H. Haji-Hashemi, P. Norouzi, M. R. Safarnejad, B. Larijani, M. M. Habibi, H. Raeisi, and M. R. Ganjali, J. Electroanal. Chem. 820 (2018) 111.
[13] F. S. Felix, and L. Angnes, Biosens. Bioelectron. 102 (2018) 470.
[14] H. Yamazoe, Mater. Sci. Eng. C (2019). doi: 10.1016/j.msec.2019.02.114.
[15] H. J. Hwang, I. Choi, Y. J. Kim, Y. K. Kim, W. S. Yeo, Coll. Surfaces B 173 (2019) 164.
[16] H. Haji-Hashemi, P. Norouzi, M. R. Safarnejad, M. R. Ganjali, Sens. Actuators B 244 (2017) 211.
[17] H. Jia, P. Gao, H. Ma, D. Wu, B. Du, and Q. Wei, Bioelectrochemistry 101 (2015) 22.
[18] S. Hassani, M. R. Akmal, A. Salek-Maghsoudi, S. Rahmani, M. R. Ganjali, P. Norouzi, and M. Abdollahi, Biosens. Bioelectron. 120 (2018) 122.
[19] S. Soukhtehzari, M. J. Rasaee, and M. Javanmardi, Int. J. Pept. Res. Ther., (2018) in press, https://doi.org/10.1007/s10989-018-9719-4.
[20] M. Paknejad, M. J. Rasaee, F. K. Tehrani, S. Kashanian, M. A. Mohagh, K. Omidfar and M. Rajabi Bazl, Hy Hybridomics. 22 (2003) 153.
[21] P. C. Abad, I. S. Mian,C. Plachot, A. Nelpurackal, C. Bator-kelly and S. A. Lelièvre, Prot. Sci. 13 (2004) 2573.
[22] P. Norouzi, M. R. Ganjali, A. Sepehri, and M. Ghorbani, Sens. Actuators B 110 (2005) 239.
[23] P. Norouzi, M. R. Ganjali, and P. Matloobi, Electrochem. Commun. 7 (2005) 333.
[24] N. Li, Y. Wang, Y. Li, W. Cao, H. Ma, D. Wu, B. Du and Q. Wei, Sens. Act. B, 202 (2014) 67.
[25] M. Hongmin, X. Zhang, X. Li, R. Li, B. Du and Q. Wei, Talanta. 143 (2015) 77.